Global analysis of Skyrme forces with higher-order density dependencies *

Zhi-Wei Zuo(左致玮) Jun-Chen Pei(裴俊琛)[1)] Xue-Yu Xiong(熊雪宇) Yi Zhu(朱怡)
State Key Laboratory of Nuclear Physics and Technology, School of Physics, Peking University, Beijing 100871, China

Abstract: The density-dependent term in Skyrme forces is essential to simulate three-body and many-body correlations beyond the low-momentum two-body interaction. We speculate that a single density term may be insufficient and a higher-order density dependent term is added. The present work investigates the influence of higher-order density dependencies based on extended UNEDF0 and SkM* forces. Global descriptions of nuclear masses and charge radii are presented. The extended UNEDF0 force gives a global rms error on binding energies of 1.29 MeV. The influence on fission barriers and equation of state are also investigated. Perspectives to improve Skyrme forces are discussed, including global center-of-mass corrections and Lipkin-Nogami pairing corrections.

Keywords: Skyrme forces, nuclear masses, nuclear energy density functional

PACS: 21.60.Jz, 21.10.Gv **DOI:** 10.1088/1674-1137/42/6/064106

1 Introduction

The Skyrme force [1] is a widely used non-relativistic phenomenological low-momentum effective nuclear force. The success of the Skyrme force is mainly attributed to its inclusion of a density-dependent term, which becomes a state-dependent in-medium interaction and simulates three-body and many-body correlations in the self-consistent mean-field framework. It is known that other bare two-body density-independent forces cannot simultaneously describe nuclear binding energies and charge radii [2]. The standard Skyrme forces adopt a single density-dependent term. Practical calculations, however, involve a wide range of densities [3], from dilute densities at nuclear surface halos to very high densities in neutron stars, and thus a single density-dependent term may be insufficient. A natural way to extend the Skyrme force is to add an additional higher-order density-dependent term. This is consistent with the order-by-order expansion of the energy density functional of atomic gases [4]. The pionless effective field theory results in a similar expression to the Skyrme energy density functional [5], which provides another clue for a higher-order density-dependent term.

In a previous study [6], we have investigated the influence of the higher-order density dependency based on the SLy4 force [7]. We demonstrated that the extended SLy4 force can generally improve the descriptions of binding energies, by reducing the rms error of global binding energies from 2.9 MeV to 2.3 MeV. The high-order density dependency can also impact the equation of state at very high densities. It is desirable to further investigate its influence based on other Skyrme forces, and to study the general behavior of the higher-order density dependency.

Today's fast calculations of the entire nuclear landscape enable us to explore the optimizations of effective nuclear forces from different perspectives. In recent years, there have been many developments to improve nuclear energy density functionals, such as UNEDF [8–10], Fyans-DFT [11], BCPM [12], SeaLL1-DFT [13], QMC-DFT [14], Gogny-HFB [15], Brussels-DFT [16], and covariant-DFT [17]. It is still a challenge to develop a highly-accurate universal nuclear energy density functional for bulk properties and dynamics. Thus, different Skyrme parameterizations have been developed to emphasize the description accuracies of nuclear masses [8], fission barriers [9] and shell structures [10], respectively. Bayesian analysis and covariant analysis to study correlations between parameters, and correlations between parameters and physical observables, can provide useful information for optimizations [18]. As well as statistical analysis, detailed studies of local fluctuations in the global description are also desirable to identify physics at specific nuclear mass regions.

There are also many efforts to go beyond the standard Skyrme force or beyond the Hartree-Fock approximation. There are many initiatives to construct nuclear energy density functionals from effective field theory and

Received 8 February 2018, Published online 4 May 2018
* Supported by National Natural Science Foundation of China (11522538)
1) E-mail: peij@pku.edu.cn

ab initio perspectives [5, 19–22]. In addition, it is known that the unrestricted Hartree-Fock framework naturally breaks all symmetries to take into account, to some extent, many-body correlations [3, 23, 24]. The broken symmetries can be restored via projection techniques, which would bring more correlations and beyond-mean-field corrections [24]. Indeed, the inclusion of collective correlation energies can significantly improve the descriptions of nuclear masses [15, 25, 26]. In this respect, the optimization of Skyrme forces, including various restoration corrections, should be systematically explored.

In this work, we have investigated the global descriptions of nuclear masses and charge radii and the influences of an additional higher-order density dependent term. There have been various extensions of Skyrme-type energy density functionals [27–32]. However, their advantages are not clear and applications are very limited. We perform fine optimizations to evaluate the prospects of the extended Skyrme forces. Our studies are based on two very different Skyrme forces: UNEDF0 [8] and SkM* [33]. UNEDF0 is best optimized for nuclear masses with a rms error of 1.455 MeV [8] and SkM* is very successful for fission barriers [34]. Then we optimize the extended UNEDF0 and SkM* forces and investigate various aspects of their performance. Furthermore, we study the global center-of-mass corrections and Lipkin-Nogami pairing corrections. These corrections are approximate restorations corresponding to the translational symmetry and the non-conservation of particle numbers, respectively. The detailed global analysis of these corrections is useful for the development of high-precision nuclear energy density functionals, which is our ultimate goal.

2 Theoretical framework

Systematic calculations in this work are based on the self-consistent deformed Skyrme-Hartree-Fock+BCS method. The Hartree-Fock equation is solved by the SKYAX code in axial-symmetric coordinate-space [35]. Considering the possible shape coexistences in some nuclei, calculations with different initial deformations have been performed. The Skyrme force includes the standard two-body interactions $v_{ij}^{(2)}$ and the density-dependent two-body interactions $v_{ij}^{(2)'}$ as,

$$V_{\rm Skyrme}=\sum_{i<j}v_{ij}^{(2)}+\sum_{i<j}v_{ij}^{(2)'}. \tag{1}$$

The standard two-body density-independent term can be written as [23],

$$\begin{aligned} v_{ij}^{(2)} =& t_0(1+x_0P_\sigma)\delta(\boldsymbol{r}_i-\boldsymbol{r}_j) \\ &+\frac{1}{2}t_1(1+x_1P_\sigma)[\delta(\boldsymbol{r}_i-\boldsymbol{r}_j)\boldsymbol{k}^2+\boldsymbol{k'}^2\delta(\boldsymbol{r}_i-\boldsymbol{r}_j)] \\ &+t_2(1+x_2P_\sigma)\boldsymbol{k'}\cdot\delta(\boldsymbol{r}_i-\boldsymbol{r}_j)\boldsymbol{k} \\ &+iW_0(\sigma_i+\sigma_j)\cdot\boldsymbol{k'}\times\delta(\boldsymbol{r}_i-\boldsymbol{r}_j)\boldsymbol{k}. \end{aligned} \tag{2}$$

In contrast to the standard spin-orbit term in SkM* [33], the spin-orbit term in UNEDF0 has been extended by including an explicit isovector degree of freedom [8]. The extended density dependent two-body interaction includes two terms, with a density dependency power factor γ and a higher-order power factor $\gamma+\frac{1}{3}$,

$$\begin{aligned} v_{ij}^{(2)'} =& \frac{1}{6}t_3(1+x_3P_\sigma)\rho(\boldsymbol{R})^\gamma\delta(\boldsymbol{r}_i-\boldsymbol{r}_j) \\ &+\frac{1}{6}t_{3E}(1+x_{3E}P_\sigma)\rho(\boldsymbol{R})^{\gamma+\frac{1}{3}}\delta(\boldsymbol{r}_i-\boldsymbol{r}_j). \end{aligned} \tag{3}$$

In the above equations, t_i, x_i are standard Skyrme parameters. In the extended forces, we introduce 2 more additional parameters t_{3E} and x_{3E}. In the SLy4 force [7] and SkM* [33], the power factor γ takes 1/6 and then we consider the next higher order power of 1/2=1/6+1/3. In the UNEDF forces, the power factors γ are around 1/3. It is useful to explore different combinations of density dependencies.

In the BCS calculations, the mixed pairing interaction is adopted as [36]:

$$V_{\rm mix}(\boldsymbol{r},\boldsymbol{r'})=v_{\rm p,n}\left(1-\frac{\rho(\boldsymbol{r})}{2\rho_0}\right)\delta(\boldsymbol{r}-\boldsymbol{r'}), \tag{4}$$

where $v_{\rm p,n}$ is the pairing strength for protons and neutrons, respectively, and ρ_0 is the saturation density 0.16 fm^{-3}. In the BCS scheme, a smooth pairing cutoff has been adopted [37]. The pairing strengths are given in Table 1.

Table 1. Pairing strengths for Skyrme Hartree-Fock calculations with UNEDF0 (and UNEDF0$_{\rm ext1}$) and SkM* (and SkM*$_{\rm ext1}$). The unit of the pairing strength is MeV fm^3.

	UNEDF0		SkM*	
	proton	neutron	proton	neutron
HF-BCS	400	340	480	450
HF-LN	260	210	305	275

Next we refit the extended Skyrme parameters for finite nuclei with the Simulated Annealing Method [38]. The fitting procedure has been described in our previous work [6]. We only refit the momentum-independent parameters, t_0, t_3, t_{3E}, x_0, x_3, x_{3E}, and keep other parameters unchanged. The momentum-independent parameters are correlated via the s-wave channel. Indeed, t_0 and t_3 are directly related through regularization as the leading-order terms for nuclear saturation properties [39]. In this way the influence of the extended higher-order density-dependent term can be clearly illustrated. The optimization should be more reliable the fewer parameters are adjusted. It is expected that the future

Table 2. The refitted parameters of the extended Skyrme forces based on UNEDF0 and SkM* forces. The units for t_0, t_3 and t_{3E} are MeV·fm^3, MeV·fm$^{3(1+\gamma)}$ and MeV·fm$^{3(\gamma+\frac{4}{3})}$, respectively. Other parameters have not been adjusted.

	UNEDF0	UNEDF0$_{\rm ext1}$	UNEDF0$_{\rm ext2}$	SkM*	SkM*$_{\rm ext1}$	SkM*$_{\rm ext2}$
t_0	−1883.6878	−2007.948	−2140.306	−2645.0	−2035.587	−2325.478
t_3	13901.948	11616.664	13869.309	15595.0	8007.383	11608.668
t_{3E}	0	3216.9303	1402.674	0	4795.359	2534.788
x_0	0.00974	−0.0494	−0.2363	0.09	0.2376	0.2358
x_3	−0.3808	−0.4722	−0.7760	0	−0.07488	0.2720
x_{3E}	0	−0.1540	1.5051	0	0.9955	−0.4692
γ	0.3219	$\frac{1}{4}$	$\frac{1}{4}$	$\frac{1}{6}$	$\frac{1}{6}$	$\frac{1}{6}$

optimization of all parameters, including momentum-dependent terms, can further improve the descriptions. The fitting procedure takes into account the binding energies of 50 nuclei across the landscape and the charge radii of 8 spherical nuclei. The obtained Skyrme parameters are given in Table 2.

3 Results and discussion

3.1 Extended parametrizations

There have been various density dependencies in Skyrme forces [40]. The power factor γ in the Skyrme force is also a parameter, ranging from 1/6 to 1. We studied the relation between the parameters t_0, t_3 and t_{3E} based on the UNEDF0 force by varying γ. In Fig. 1, with increasing γ, t_3 increases and t_{3E} decreases. We see that t_0 increases slightly with increasing γ. If γ is 1/3, the obtained t_{3E} becomes slightly negative, -160.389. In the original UNEDF0, γ is 0.3219, and in this case we say that t_{3E} is zero, being consistent with the systematic behavior of t_{3E}. This trend indicates that even higher-order density dependent terms would become negative, as also obtained in Ref. [41]. In Fig. 1, with a very small γ, on the other hand, the t_{3E} term dominates and the t_3 term is reduced. Note that this trend is obtained by fitting finite nuclei. UNEDF0 is obtained by the optimization of the free parameter γ and then the t_{3E} term is eliminated. In the extended UNEDF0 force, we have another parameter x_{3E} and this additional isospin degree of freedom can improve the Skyrme force, as demonstrated in the following. In contrast to the SLy4 and SkM* forces, which have γ=1/6, UNEDF0, with γ around 1/3, has little room for a higher-order density dependent term. By comparing the values of t_3 and t_{3E}, we assume that in a reasonable combination, t_{3E}, as a higher-order term, should be smaller than t_3. Therefore we take γ as 1/4 to refit the extended UNEDF0 force, in which the power factor of the higher-order term is 1/4+1/3=7/12. The optimized extended Skyrme forces are given in Table 2.

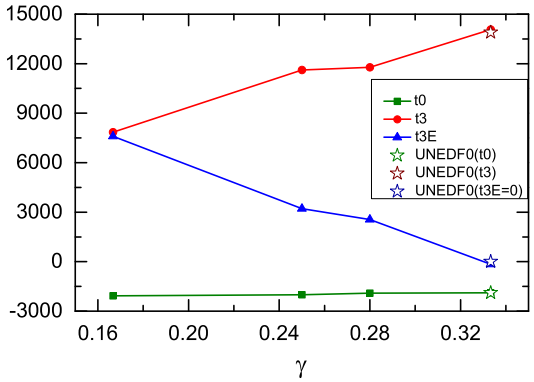

Fig. 1. (color online) The refitted parameters t_0, t_3 and t_{3E} of the extended UNEDF0 force are given as function of the power factor γ. The parameters of the original UNEDF0 force are shown as stars.

3.2 Global binding energies

To evaluate the influence of the additional density dependent term, we refit the extended UNEDF0 force. With the optimized UNEDF0$_{\rm ext1}$ force, we did global studies of nuclear ground state properties based on Skyrme-Hartree-Fock+BCS calculations. Figure 2 displays the binding energy differences between theoretical calculations and experimental data for 603 even-even known nuclei. UNEDF0 has been optimized on a large scale for binding energies, with a global rms error of 1.455 MeV for 520 even-even nuclei [8]. This is the best description of binding energies with the standard Skyrme force. In our Hartree-Fock+BCS calculations of 603 nuclei, the global rms values of UNEDF0 and UNEDF0$_{\rm ext1}$ are 1.503 and 1.316 MeV, respectively. We see the additional higher-order density dependent term can reduce the rms by 12%. For the region $A\leqslant 80$, the rms is 1.58 MeV. For the region $A> 80$, the rms is 1.23 MeV. We do not refit the UNEDF0 force, since it has been extremely optimized [8]. In the region of heavy nuclei, we see the discrepancies between theoretical and experimental values are dominated by the overestimated shell effects. The UNEDF0$_{\rm ext1}$ has slightly adjusted the balance between the ^{208}Pb region and the deformed neutron-rich region

around ^{178}Yb, ^{182}Hf and ^{186}W. In light nuclei, one of the main discrepancies is from the $N = Z$ nuclei. We see that both theoretical calculations generally underestimate the binding energies of these self-conjugated light nuclei and overestimate the binding energies of drip-line light nuclei. This can be explained as clustering effects and *np*-correlations are absent in the Skyrme-Hartree-Fock framework. Indeed the valence n-p interactions of $N=Z$ light nuclei have been remarkably underestimated by the nuclear density functional theory [42].

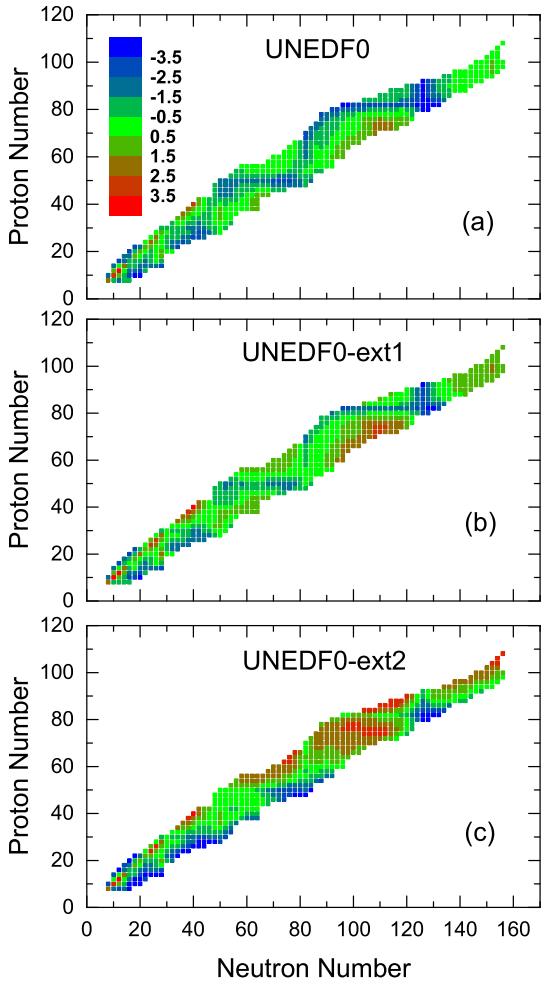

Fig. 2. (color online) The binding energy differences between theoretical calculations and experimental data [43] for 603 even-even nuclei, given as $E_{\rm B}^{\rm Calc.}$–$E_{\rm B}^{\rm Expt.}$ in MeV. The results are obtained by Hartree-Fock+BCS calculations with (a) UNEDF0, (b) UNEDF0$_{\rm ext1}$, and (c) UNEDF0$_{\rm ext2}$. See Table 2 for the parameter sets.

Figure 3 displays the global studies of binding energies of SkM* and extended SkM* forces. The SkM* force [33] has been widely used for fission studies due to its small surface-energy coefficient. In Fig. 3(a), we see the SkM* force is not good at descriptions of global binding energies, and the rms of binding energies is 6.305 MeV. It overestimates the binding energies of neutron-rich light and medium nuclei and underestimates the binding energies of proton-rich heavy and superheavy nuclei.

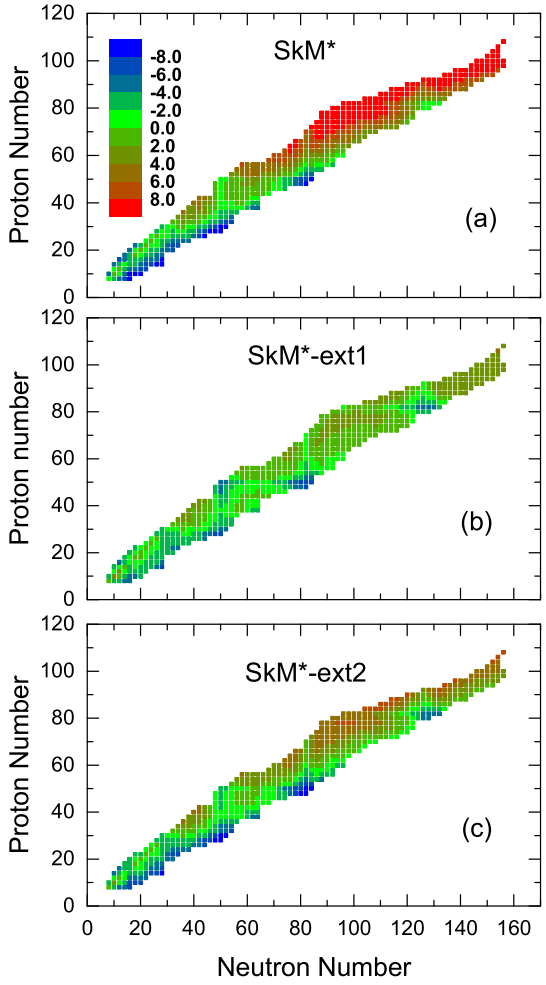

Fig. 3. (color online) The binding energy differences between calculations and experiments [42] for 603 even-even nuclei, given as $E_{\rm B}^{\rm Calc.} - E_{\rm B}^{\rm Expt.}$ in MeV. The results are obtained by Hartree-Fock+BCS calculations with (a) SkM*, (b) SkM$^*_{\rm ext1}$, and (c) SkM$^*_{\rm ext2}$. See Table 2 for the parameter sets.

In Fig. 3(b), we refit SkM* with the the higher-order density dependent term as SkM$^*_{\rm ext1}$. We see that the SkM$^*_{\rm ext1}$ descriptions of binding energies have been much improved, with a rms error of 2.358 MeV. We see again similar features between SkM$^*_{\rm ext1}$ and UNEDF0$_{\rm ext1}$ results. The binding energies of light neutron-rich nuclei are overestimated and the binding energies of some $N=Z$ nuclei are underestimated. The predicted neutron drip-line in the light and medium mass region could therefore be overextended by the SkM* force.

3.3 Fission barriers

It has been a long-standing goal to simultaneously and accurately describe nuclear masses and fission barriers. It is known that SkM* is good at descriptions of fission barriers and UNEDF0 is good at descriptions of nuclear masses. In Fig. 2(c) and Fig.3(c), we refit the extended UNEDF0 and SkM* with the input of the fission isomer energy of ^{240}Pu. The isomer energy is defined by the binding energy difference between the ground state and the fission isomer. The obtained extended Skyrme forces are UNEDF0$_{\rm ext2}$ and SkM$^*_{\rm ext2}$, respectively, as listed in Table 2. We see that the UNEDF0$_{\rm ext2}$ and SkM$^*_{\rm ext2}$ descriptions of binding energies become worse again with rms errors of 1.87 MeV and 3.676 MeV, respectively. This demonstrates that there is a competition in the simultaneous optimization of nuclear masses and fission barriers (or surface properties). We see that SkM* , SkM$^*_{\rm ext2}$ and UNEDF0$_{\rm ext2}$ forces which have been fitted with fission barriers have all significantly underestimated binding energies of proton-rich heavy nuclei and overestimated binding energies of neutron-rich light nuclei, implying conflicting isospin-dependent corrections on binding energies and fission barriers. Such a competition has also been reflected in the increased rms values of 1.91 MeV of UNEDF1 [9] compared to the 1.455 MeV of UNEDF0 [8], in which the optimization of UNEDF1 includes both fission isomers and nuclear masses, while the optimization of UNEDF0 does not include fission isomers.

Figure 4 displays the calculated symmetric fission barriers of ^{240}Pu with the extended UNEDF0 and SkM* forces. The triaxial deformation and reflection-asymmetric deformation, which are important for descriptions of fission barriers, have not been considered. In principle, multi-dimensional constraint calculations should be performed to study fission barriers [44, 45]. Nevertheless it is suitable to consider the fission isomer energies in the symmetric case to constrain large deformation properties to reduce computing time. The experimental excitation energy of the fission isomer of ^{240}Pu is 2.8 MeV [46]. In our case, the fission isomer energies of ^{240}Pu calculated by UNEDF0, UNEDF0$_{\rm ext1}$ and UNEDF0$_{\rm ext2}$ are 4.95, 4.99, 4.23 MeV, respectively. The fission isomer energies of ^{240}Pu calculated by SkM*, SkM$^*_{\rm ext1}$ and SkM$^*_{\rm ext2}$ are 2.65, 4.2, 3.44 MeV, respectively. We see the fission barrier heights are significantly overestimated at large deformations with nuclear forces which are good at descriptions of nuclear masses. It is difficult to obtain a satisfactory parameterization for fission barriers based on the extended UNEDF0 force by adjusting only the momentum-independent parameters. In addition, the pairing interaction strength can also affect the fission barriers [47], which can be reduced by increasing the pairing strengths.

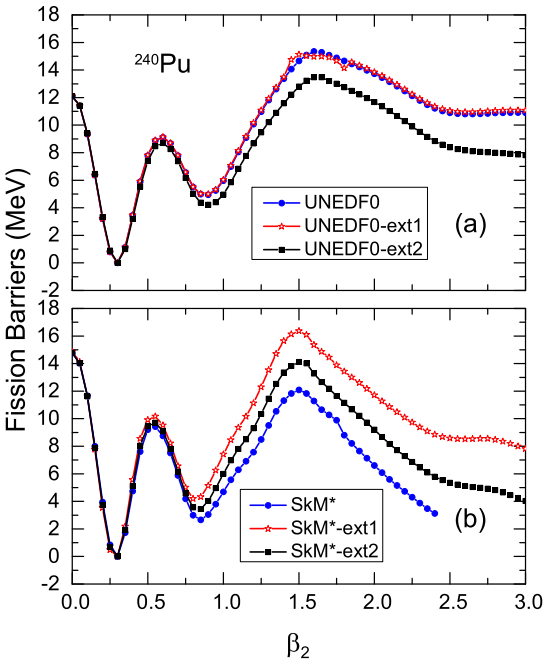

Fig. 4. (color online) Calculated symmetric fission barriers of ^{240}Pu as a function of quadrupole deformation β_2 with extended Skyrme forces: (a) with UNEDF0, UNEDF0$_{\rm ext1}$, and UNEDF0$_{\rm ext2}$ forces; and (b) with SkM*, SkM$^*_{\rm ext1}$, and SkM$^*_{\rm ext2}$ forces. The parameters are listed in Table 2.

3.4 Global charge radii

The charge radius is also an important bulk observable associated with nuclear saturation properties. For example, the systematic studies of charge radii of Ca isotopes have recently been a hot topic [48], providing a chance to look for the evolution of shell structures and deformations. There are extensive studies of global binding energies. There are fewer experimental data for charge radii than for binding energies, however. Fortunately, the method using laser isotope shifts is very precise for measurements of charge radii of ground states and isomeric states [48].

Figure 5 displays the global calculations of charge radii of 339 even-even nuclei compared to experimental data [49]. With the refitted UNEDF0$_{\rm ext1}$ and SkM$^*_{\rm ext1}$ forces, the obtained charge radii rms are 0.027 fm and 0.023 fm respectively. Actually the original Skyrme forces and the extended Skyrme force are very close in descriptions of charge radii. We see that SkM$^*_{\rm ext1}$ descriptions of charge radii are slightly better than those of UNEDF0$_{\rm ext1}$. Both descriptions of charge radii of light nuclei are unsatisfactory. The UNEDF0 and UNEDF0$_{\rm ext1}$ forces are not good at descriptions of charge radii around ^{102}Zr. Generally the descriptions of charge radii of light nuclei are less satisfactory than those of heavy nuclei. There are no significant shell effects in

the descriptions of charge radii in contrast to binding energies. There are several specific regions that neither parametrizations can describe well. For example, large discrepancies are identified in ^{16}O, ^{20,28}Ne, ^{24}Mg, ^{48}Ca, ^{146,150}Dy, ^{192,194,216,218}Po and $^{242-248}$Cm. These distinct discrepancies should be considered in the future optimizations of Skyrme forces.

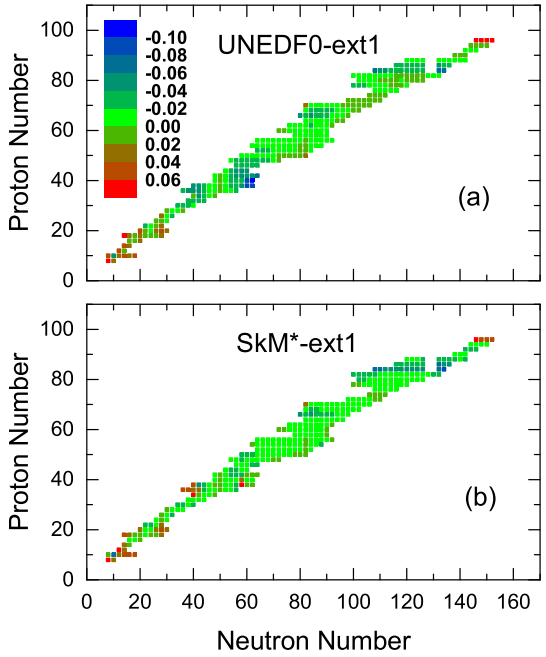

Fig. 5. (color online) The charge radii of 339 even-even nuclei are calculated by the Skyrme-Hartree-Foc+BCS method with UNEDF0$_{\rm ext1}$ and SkM$^*_{\rm ext1}$ forces. The differences between calculated values and experimental data, $R^{\rm Calc.}$-$R^{\rm Expt.}$, are displayed. The unit of charge radii is fm.

3.5 Equation of state

In our previous work [6], we have shown that the higher-order density-dependent term can particularly affect the equation of state in the high density region. The equation of state in the high density region is critical to address the properties of neutron stars. Figure 6 displays the pressure of symmetric nuclear matter as a function of densities, which are obtained from the extended SkM* forces. Generally, it can be seen that the pressure from the extended forces increases in the high density region compared to the original forces. This is consistent with our previous results based on the extended SLy4 force [6]. The differences between UNEDF0$_{\rm ext1}$, UNEDF0$_{\rm ext2}$ and UNEDF0 are very small and are not shown. At the saturation point, the incompressibilities of the extended forces slightly increase.

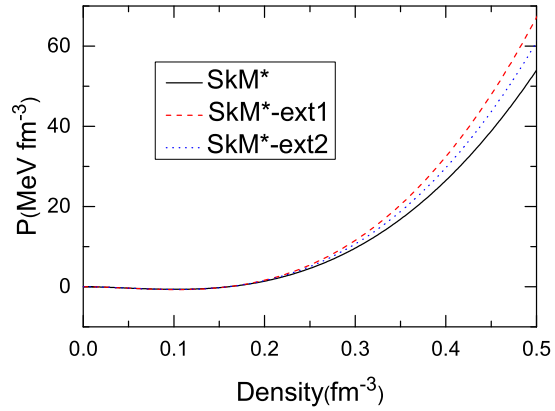

Fig. 6. (color online) Pressure of symmetric nuclear matter as a function of densities, obtained with SkM*, SkM$^*_{\rm ext1}$, and SkM$^*_{\rm ext2}$ forces.

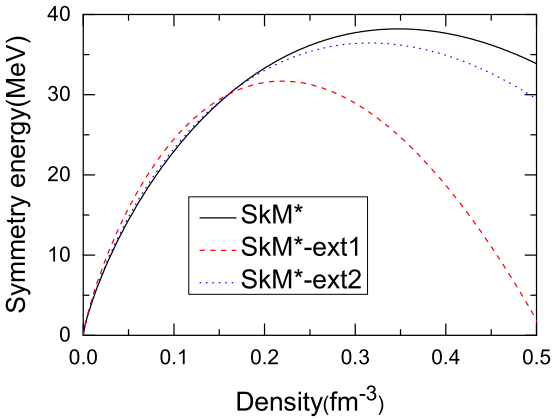

Fig. 7. (color online) Symmetry energy of the symmetric nuclear matter as a function of densities, obtained with SkM*, SkM$^*_{\rm ext1}$, and SkM$^*_{\rm ext2}$ forces.

Figure 7 displays the symmetry energies as a function of densities. Generally, it can be seen that the symmetry energies of the extended forces decrease at high density region compared to the original forces. This is also consistent with our previous results based on SLy4 [6]. Note that the symmetry energy at the saturation point has not been adjusted. Our results show that the symmetry energies at high densities consistently become soft, and this has been indicated by the experimental π^-/π^+ ratio [50], although soft symmetry energies at high densities are still controversial. In both Fig. 6 and Fig. 7, the equation of state from SkM$^*_{\rm ext2}$, which is refitted with inputs of fission barriers, is between SkM* and SkM$^*_{\rm ext1}$. The symmetry energy of the extended force at the saturation point is unchanged in the fitting procedure, while the slope is changed. In particular, the slope of symmetry energy L of UNEDF0$_{\rm ext2}$ (L=51.8 MeV) is larger than that of UNEDF0 (L=45 MeV) and UNEDF0$_{\rm ext1}$ (L=45.4 MeV). The slopes of symmetry energy of SkM*

(L=45.8 MeV)and SkM$^*_{\rm ext2}$ (L=42.5 MeV) are larger than that of SkM$^*_{\rm ext1}$(L=27.5 MeV). This indicates that the fitting including fission barriers tends to increase the slope of symmetry energy.

3.6 Global center-of-mass corrections

Before we develop the next-generation effective nuclear forces, we should comprehensively understand the beyond mean-field corrections. Symmetries in unrestricted density functional theory are spontaneously broken to account for many-body correlations. Correspondingly, there are various projection methods to restore the broken symmetries [3]. For example, the center-of-mass correction is used to restore the translation symmetry, the angular momentum projection is used to restore the rotation symmetry, and the particle number projection is used to restore the gauge symmetry due to pairing.

The center-of-mass correction is in principle important in light nuclei and in *ab initio* calculations [51]. It has been demonstrated to be important for descriptions of nuclear surface properties [52]. On the other hand, the optimized density functional theory can give good descriptions of fission barriers [9]. It is desirable to study the global center-of-mass corrections. The center-of-mass (c.m.) correction energy includes the diagonal term (one-body) and the off-diagonal term (two-body) [52] as:

$$E_{\rm c.m.}=\frac{1}{2mA}\sum_{i=1}^{A}\boldsymbol{P}_i^2+\frac{1}{2mA}\sum_{i>j}\boldsymbol{P}_i\cdot\boldsymbol{P}_j \qquad (5)$$

Figure 8 displays the global off-diagonal c.m. corrections, which are actually comparable to the diagonal c.m. contributions but with the opposite sign. Note that systematic calculations of c.m. corrections with standard Skyrme forces have been performed in Refs. [52, 53]. It can be seen that the shell effects and isospin dependencies in the c.m. corrections are not significant for both UNEDF0$_{\rm ext1}$ and SkM$^*_{\rm ext1}$ forces. For UNEDF0$_{\rm ext1}$, the smooth two-body c.m. contributions can be refitted roughly as $4.05A^{0.216}$. Note that the one-body diagonal c.m. corrections can be fitted roughly as $-14.58A^{0.047}$, which is almost mass-independent. The total c.m. correction can be fitted as $-18.33A^{-0.208}$. For SkM$^*_{\rm ext1}$, the one-body and two-body corrections can be fitted as $-14.916A^{0.046}$ and $4.20A^{0.211}$ respectively, and the total c.m. correction is $-18.61A^{-0.213}$. We see the two different Skyrme forces have very close c.m. corrections. For A<40, the off-diagonal c.m. corrections deviate from the fitted functions, indicating that microscopic c.m. corrections play a special role in light nuclei.

In Ref. [52], it has been pointed out that the c.m. correction is closely related to surface energies. The role of surface energies associated with Skyrme forces has been extensively studied [54]. In our calculations, the two-body term is a function of $A^{0.2}$, which is close to the surface curvature term rather than the surface term. The inclusion of the curvature term in the liquid drop model can indeed remarkably improve the description of fission barriers, although it is not essential for descriptions of binding energies [55]. It is still a puzzle that the curvature coefficient from the leptodermous expansion in self-consistent calculations is much larger than in the liquid drop model [53, 56]. Based on our results, *a posteriori* two-body c.m. correction can significantly reduce the curvature coefficient in microscopic calculations. We see that the one-body and two-body c.m. corrections have very different nuclear mass dependencies. This may imply a mass-dependent nuclear force if only the one-body c.m. correction is included. The simultaneous optimization of Skyrme forces for both binding energies and fission barriers has not been satisfied so far. It is controversial that the fission barriers of actinide nuclei are mainly correlated with the surface symmetry energy rather than the surface curvature energy [57]. Our results demonstrate that the off-diagonal c.m. correction is related to the surface curvature energy and thus is important for descriptions of surface properties, which is beyond the optimizations of Skyrme forces with only diagonal c.m. corrections.

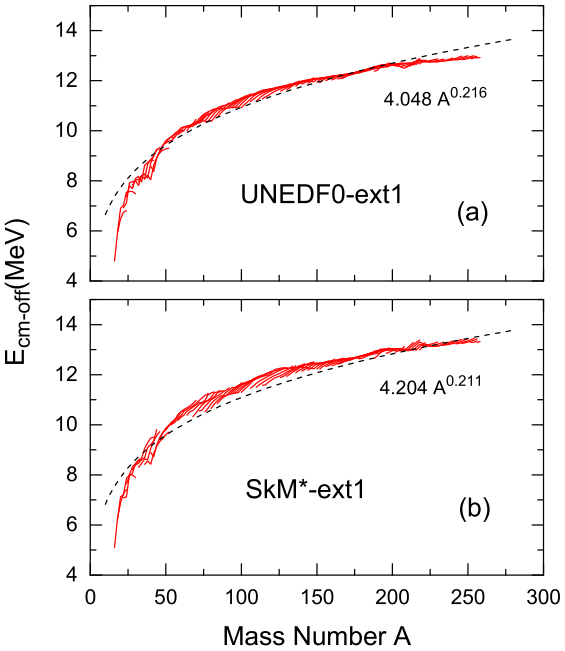

Fig. 8. (color online) Off-diagonal center-of-mass corrections obtained by deformed Skyrme-Hartree-Fock+BCS calculations with (a) UNEDF0$_{\rm ext1}$ and (b) SkM$^*_{\rm ext1}$. The fitted functions are given as dashed lines.

3.7 Global Lipkin-Nogami corrections

The pairing correlations in nuclei can be treated by BCS or Bogoliubov approximations in the framework of

independent quasiparticle particles, which is associated with the spontaneous breaking of the gauge symmetry and the non-conservation of particle numbers. For simplicity, the Lipkin-Nogami method [58, 59] is usually adopted to conserve the particle numbers at the order of $(\Delta N)^2$. To demonstrate the effects of Lipkin-Nogami (LN) corrections, we display the binding energy differences between the Hartree-Fock-BCS (HF-BCS) and Hartree-Fock-LN (HF-LN) methods,

$$\Delta E_{\rm LN}=E_{\rm HF-LN}-E_{\rm HF-BCS}. \quad (6)$$

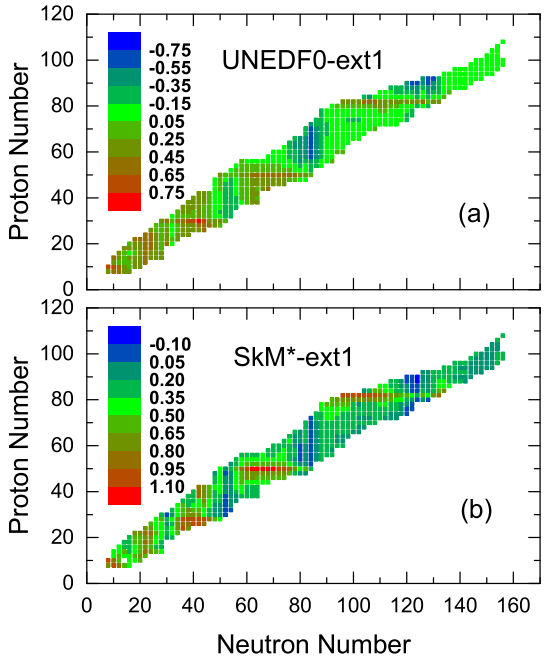

Fig. 9. (color online) The comparison of binding energies between Hartree-Fock-Lipkin-Nogami and Hartree-Fock-BCS calculations with different Skyrme forces, for (a) UNEDF0$_{\rm ext1}$, and (b) SkM$^*{}_{\rm ext1}$.

Figure 9 displays the global LN corrections of $\Delta E_{\rm LN}$, which are calculated with UNEDF0$_{\rm ext1}$ and SkM$^*{}_{\rm ext1}$ forces and mixed-pairing interactions. The pairing strengths adopted by the two approaches in this work have been adjusted to reproduce the pairing gaps in ^{252}Fm, as listed in Table 1. The adjusted LN pairing strengths are slightly smaller than the BCS pairing strengths. The proton pairing strengths are slightly larger than the neutron pairing strengths. The pairing strengths for UNEDF0$_{\rm ext1}$ are smaller than in SkM$^*{}_{\rm ext1}$ due to a larger effective mass. It can be seen that generally the binding energy differences are within 0.75 MeV for UNEDF0$_{\rm ext1}$ and are less than 1.1 MeV for SkM$^*{}_{\rm ext1}$. It is evident that the global LN corrections are related to shell structures. The global patterns of LN corrections with the two Skyrme forces are very similar. Compared to the BCS approximation, the LN approximation gives higher binding energies for neutron shell gaps than proton shell gaps. For light nuclei, the features of LN corrections are complex. The earlier study has pointed out that statistically, the restoration of the exact particle number does not significantly improve the global descriptions of nuclear masses [60]. In our calculations with UNEDF0$_{\rm ext1}$, the rms of binding energies with the HF-LN approach is 1.291 MeV, which is slightly better than the HF-BCS approach of 1.316 MeV. For SkM$^*{}_{\rm ext1}$, the rms errors of HF-LN and HF-BCS are almost the same.

4 Summary

In summary, we have studied the global performance of Skyrme forces with an extended higher-order density-dependent term. Our studies are based on two very different Skyrme forces: UNEDF0, which is optimized for nuclear masses, and SkM*, which is optimized for fission barriers. We only adjusted the momentum-independent parameters. The global descriptions of binding energies with UNEDF0$_{\rm ext1}$ have obtained a rms of 1.29 MeV, which is encouraging, compared to the best-optimized UNEDF0 rms of 1.455 MeV. In addition, the systematic analysis demonstrated that the binding energies of $N=Z$ nuclei have generally been underestimated. The descriptions of charge radii are generally good except in some local regions.

We demonstrated that there is a competition in the simultaneous optimization of binding energies and fission barriers. In this respect, our systematic calculations demonstrated that the off-diagonal center-of-mass corrections are numerically related to the surface curvature energy rather than the surface energy, which is important for proper description of surface properties and should be included in future optimizations. The features of the Lipkin-Nogami pairing corrections with two Skyrme forces are very similar and are related to shell gaps. Statistically, the Lipkin-Nogami method cannot significantly improve the descriptions of global binding energies. We have not yet studied the rotational corrections related to deformations, which involve configuration mixtures and are more complicated. These microscopic corrections may be linked to the phenomenological corrections in high-precision nuclear mass models [61]. We also studied the influence of the high-order density dependent term on the equation of state. It mainly impacts the high-density properties, consistent with our previous study based on the SLy4 force. The higher-order density dependent term has a large impact on Skyrme forces with a small power factor γ, such as SLy4 and SkM* forces. At present we have only adjusted the momentum-independent parameters based on existing Skyrme forces. The optimization of extended Skyrme forces with all parameters is in progress and the perfor-

mance is expected to be further improved. Our global analysis should be useful for the future development of high-precision nuclear energy density functionals.

The computation for this work was performed on the Tianhe-1A supercomputer in Tianjin and the Tianhe-2 supercomputer in Guangzhou.

References

1 T. H. R. Skyrme, Phil. Mag., **1**: 1043 (1956)
2 J. W. Negele, Rev. Mod. Phys., **54**: 913 (1982)
3 M. Bender, P.-H. Heenen, and P.-G. Reinhard, Rev. Mod. Phys., **75**: 121 (2003)
4 K. Huang and C. N. Yang, Phys. Rev., **105**: 767 (1957); T. D. Lee and C. N. Yang, Phys. Rev., **105**: 1119 (1957); P. Martin and C. De Dominicis, Phys. Rev., **105**: 1417 (1957)
5 R. J. Furnstahl, Lecture Notes in Physics, Vol.852, 133 (Springer-Verlag, 2012)
6 X. Y. Xiong, J. C. Pei, and W. J. Chen, Phys. Rev. C, **93**: 024311 (2016)
7 E. Chabanat, P. Bonche, P. Haensel, J. Meyer, and R. Schaeffer, Nucl. Phys. A, **635**: 231 (1998)
8 M. Kortelainen, T. Lesinski, J. Moré, W. Nazarewicz, J. Sarich, N. Schunck, M. V. Stoitsov, and S. Wild, Phys. Rev. C, **82**: 024313 (2010)
9 M. Kortelainen, J. McDonnell, W. Nazarewicz, P.-G. Reinhard, J. Sarich, N. Schunck, M. V. Stoitsov, and S. M. Wild, Phys. Rev. C, **85**: 024304 (2012)
10 M. Kortelainen, J. McDonnell, W. Nazarewicz, E. Olsen, P.-G. Reinhard, J. Sarich, N. Schunck, S. M. Wild, D. Davesne, J. Erler, and A. Pastore, Phys. Rev. C, **89**: 054314 (2014)
11 S. V. Tolokonnikov, I. N. Borzov, M. Kortelainen, Yu. S. Lutostansky, and E. E. Saperstein, J. Phys. G, **42**: 075102 (2015)
12 M. Baldo, L. M. Robledo, P. Schuck, and X. Vinas, Phys. Rev. C, **87**: 064305(2013)
13 A. Bulgac, M. M. Forbes, S. Jin, R. N. Perez, and N. Schunck, arXiv:1708.08771
14 J. R. Stone, P. A. M. Guichon, P. G. Reinhard, and A. W. Thomas, Phys. Rev. Lett., **116**: 092501 (2016)
15 S. Goriely, S. Hilaire, M. Girod, and S. Peru, Phys. Rev. Lett., **102**: 242501 (2009)
16 S. Goriely, N. Chamel, and J. M. Pearson, Phys. Rev. C, **88**: 024308 (2013)
17 P. W. Zhao, Z. P. Li, J. M. Yao, and J. Meng, Phys. Rev. C, **82**: 054319 (2010)
18 J.D. McDonnell, N. Schunck, D. Higdon, J. Sarich, S.M. Wild, and W. Nazarewicz, Phys. Rev. Lett., **114**: 122501 (2015)
19 M. Grasso, D. Lacroix, and U. van Kolck, Phys. Scr., **91**: 063005 (2016)
20 J. Dobaczewski, J. Phys. G, **43**: 04LT01 (2016)
21 T. Duguet, M. Bender, J. -P. Ebran, T. Lesinski, and V. Somà, Eur. Phys. J. A, **51**: 162 (2015)
22 M. Stoitsov, M. Kortelainen, S. K. Bogner, T. Duguet, R. J. Furnstahl, B. Gebremariam, and N. Schunck, Phys. Rev. C, **82**: 054307 (2010)
23 P. Ring and P. Schuck, The nuclear many-body problem, (Springer, Berlin), 1980
24 C. Yannouleas and U.Landman, Rep. Prog. Phys., **70**: 2067 (2007)
25 K. Q. Lu, Z. X. Li, Z. P. Li, J. M. Yao, and J. Meng, Phys. Rev. C, **91**: 027304 (2015)
26 P. Klupfel, J.Erler, P.-G.Reinhard, and J. A. Maruhn, Eur. Phys. J. A, **37**: 343 (2008)
27 M. Waroquier, J. Sau, and K. Heyde, Phys. Rev. C, **19**: 1640 (1983)
28 A. K. Dutta, J. -P.Arcoragi, J. M. Pearson, R. Behrman, and F. Tondeur, Nucl. Phys. A, **458**: 77 (1986)
29 Michel Farine, J. M. Pearson, and F. Tondeur, Nucl. Phys. A, **615**: 135 (1997)
30 T. Lesinski, K. Bennaceur, T. Duguet, and J. Meyer, Phys. Rev. C, **74**: 044315 (2006)
31 B. Cochet, K. Bennaceur, P. Bonche, T. Duguet, and J. Meyer, Nucl. Phys. A, **731**: 34 (2004)
32 B. K. Agrawal, Shashi K. Dhiman, and Raj Kumar, Phys. Rev. C, **73**: 034319 (2006)
33 J. Bartel, P. Quentin, M. Brack, C. Guet, and H. B. Håkansson, Nucl. Phys. A, **386**: 79 (1982)
34 A. Staszczak, A. Baran, and W. Nazarewicz, Phys. Rev. C, **87**: 024320 (2013)
35 P.-G. Reinhard, computer code SKYAX (unpublished)
36 J. Dobaczewski, W. Nazarewicz, and M. V. Stoitsov, Eur. Phys. J. A, **15**: 21 (2002)
37 M. Bender, K. Rutz, P.-G. Reinhard, and J. A. Maruhn, Eur. Phys. J. A, **8**: 59 (2000)
38 Available at http://jblevins.org/mirror/amiller/simann.f90
39 C.-J. Yang, M. Grasso, and D. Lacroix, Phys. Rev. C, **96**: 034318 (2017)
40 J. R. Stone, P.-G. Reinhard, Prog. Part. Nucl. Phys., **58**: 587 (2007)
41 B. K. Agrawal, S. Shlomo, and V. Kim Au, Phys. Rev. C, **72**: 014310 (2005)
42 G. Audi, M. Wang, A. H. Wapstra, F. G. Kondev, M. MacCormick, X. Xu, and B. Pfeiffer, Chin. Phys. C, **36**: 1287 (2012)
43 M. Stoitsov, R. B. Cakirli, R. F. Casten, W. Nazarewicz, and W. Satula, Phys. Rev. Lett., **98**: 132502 (2007)
44 B.-N. Lu, E.-G. Zhao, and S.-G. Zhou, Phys. Rev. C, **85**: 011301(R) (2012)
45 B.-N. Lu, J. Zhao, E.-G. Zhao, and S.-G. Zhou, Phys. Rev. C, **89**: 014323 (2014)
46 B. Singh, R. Zywina, and R. B. Firestone, Nucl. Data Sheets, **97**: 241 (2002)
47 S. Karatzikos, A. V. Afanasjev, G. A. Lalazissis, and P. Ring, Phys. Lett. B, **689**: 72 (2010)
48 R. F. Garcia Ruiz et al, Nature Physics, **12**: 594 (2016)
49 I. Angeli, K. P. Marinova, At. Data. Nucl. Data. Tab., **99**: 69 (2013)
50 Z. G. Xiao, B. A. Li, L. W.Chen, G. C.Yong, and M. Zhang, Phys. Rev. Lett., **102**: 062502 (2009)
51 P. Maris, J. P. Vary, and A. M. Shirokov, Phys. Rev. C, **79**: 014308 (2009)
52 M. Bender, K. Rutz, P.-G. Reinhard, and J.A. Maruhn, Eur. Phys. J. A, **7**: 467 (2000)
53 P.-G. Reinhard, M. Bender, W. Nazarewicz, and T. Vertse, Phys. Rev. C, **73**: 014309 (2006)
54 R. Jodon, M. Bender, K. Bennaceur, and J. Meyer, Phys. Rev. C, **94**: 024335 (2016)
55 K. Pomorski and J. Dudek, Phys. Rev. C, **67**: 044316 (2003)
56 M. Durand, P. Schuck, X. Vinas, Z. Phys. A, **346**: 87 (1993)
57 N. Nikolov, N. Schunck, W. Nazarewicz, M. Bender, and J. Pei, Phys. Rev. C, **83**: 034305 (2011)
58 H. J. Lipkin, Ann. Phys., **9**: 272 (1960)
59 Y. Nogami, Phys. Rev., **134**: B313 (1964)
60 M. Samyn, S. Goriely, M. Bender, and J. M. Pearson, Phys. Rev. C, **70**: 044309 (2004)
61 S. Goriely, M. Samyn, and J. M. Pearson, Phys. Rev. C, **75**: 064312 (2007)